American Mineralogist, Volume 63, pages 1137–1142, 1978

The crystal chemistry and petrogenesis of a magnesian rhodonite[1]

DONALD R. PEACOR, ERIC J. ESSENE, PHILIP E. BROWN AND GARY A. WINTER

Department of Geology and Mineralogy, The University of Michigan
Ann Arbor, Michigan 48109

Abstract

Rhodonite with unusually high magnesium and low iron contents, $Mn_{3.73}Mg_{0.73}Ca_{0.51}Fe_{0.03}Si_5O_{15}$, occurs in a metamorphosed sedimentary evaporite sequence at Balmat, New York. It coexists with an unusual pyroxene having average composition close to $MnMgSi_2O_6$, talc, calcite, and a number of other minerals. Refinement of the crystal structure using single-crystal X-ray diffraction data shows that Mg has a marked preference for the M4 site ($Mg_{0.47}Mn_{0.53}$), and that M1, M2, and M3 have nearly equal Mg occupancies of slightly more than 0.1. Relations with coexisting phases indicate that both the Mg content and degree of ordering of Mg in M4 are near the maximum to be expected for naturally occurring rhodonite.

Introduction

Two samples of rhodonite were found by miners in different areas of the Balmat Mine No. 4, and saved only because of their attractive appearance and uniqueness. Portions of each sample were kindly made available to us by Dr. Dill of the mine staff, and we refer to them simply as samples 1 and 2, respectively. The rhodonite of sample 1 occurs with a pyroxene of approximate composition $MnMgSi_2O_6$ which is currently under investigation, and fine-grained talc and quartz. The second sample also has both rhodonite and the pyroxene, but also contains barite, anhydrite, manganoan calcite, apatite, quartz, hauerite, and a phase tentatively identified as datolite. These two samples were recovered from interlayered metasediments (evaporites) consisting largely of talc, tremolite, calcite, and anhydrite, which are the host rocks for the ore body. The deposit has been regionally metamorphosed with estimated conditions of $P = 6.5 \pm 0.5$ kbar, $T = 625 \pm 25$°C (Brown *et al.*, 1978). The conditions for equilibration of rhodonite and its coexisting phases are thus reasonably well-defined.

Preliminary energy-dispersive analyses using the electron microprobe revealed that the rhodonite was unusually rich in Mg and poor in Fe. Quantitative spectrometer analyses were therefore obtained for rhodonite from both samples, and the results are presented in Table 1. Single-crystal X-ray diffraction confirmed that the analyzed material had the rhodonite structure. Because this rhodonite has a Mg content greater than that of most other rhodonites, and because the iron content is exceptionally low, we concluded that a structure refinement would provide definitive data regarding the occupancy of Mg over the octahedral sites.

X-ray diffraction data

Unit-cell parameters were determined by least-squares refinement, with data for nineteen reflections obtained from a powder diffractometer pattern as corrected with quartz as an internal standard. The parameters are $a = 9.797(3)$, $b = 10.497(3)$, $c = 12.185(4)$A, $\alpha = 108.55(4)$, $\beta = 103.02(4)$, $\gamma = 82.49(4)°$. The space group is $C\bar{1}$. We use this setting, recommended by Ohashi and Finger (1975), as well as the atom nomenclature of those authors, because it provides a more direct means of comparing pyroxenoid structures. Powder diffractometer data are listed in Table 2.

Intensity data were obtained from a cleavage fragment measuring approximately $0.15 \times 0.20 \times 0.40$ mm, mounted for rotation about the c axis on the Weissenberg-geometry diffractometer. Mo$K\alpha$ radiation, monochromated with a flat graphite crystal and detected with a scintillation counter, was used. The Supper-Pace automated system was used, employing

[1] Contribution No. 341 from the Mineralogical Laboratory, Department of Geology and Mineralogy, The University of Michigan.

0003–004X/78/1112–1137$02.00

Table 1. Electron microprobe analysis of magnesian rhodonite[1]

Oxide	wt. %	Molar ratio/5 Si
SiO_2	47.66	5.00
Al_2O_3	0.06	0.00
MnO	42.62	3.73
MgO	4.72	0.73
FeO	0.37	0.03
CaO	4.58	0.51
sum	99.99	

[1]Standards used were synthetic tephroite for Mn, ANU rhodonite for Si, Irving kaersutite for Al, Ca, Fe, Mg. Drift, atomic number, fluorescence, absorption and background corrections were applied to the data.

a scan across each reflection with background measured on each side. A total of 2473 intensities were measured, of which 152 were unobserved, up to a $\sin\theta$ limit of 0.46 and an l index limit of 13. All intensities were corrected for Lorentz-polarization and absorption effects (μ = 51.5 cm^{-1}). A modified version of a program ABSRP written by C. W. Burnham was used for the absorption correction.

Table 2. X-ray power diffraction data[1]

hkl	d(calc)	d(obs)	I	hkl	d(calc)	d(obs)	I
110*	7.105	7.1	50	33$\bar{4}$	2.260	2.259	3
1$\bar{1}$0*	6.666	6.67	15	330	2.222		
200*	4.763	4.76	50	20$\bar{5}$	2.221	2.220	24
021*	4.118	4.12	8	40$\bar{3}$*	2.220		
201	4.113			223	2.220		
112	3.811	3.81	15	331	2.207	2.208	8
22$\bar{1}$	3.802			24$\bar{1}$*	2.178	2.178	53
02$\bar{3}$	3.562	3.55	85	33$\bar{1}$	2.154	2.152	6
220*	3.552			3$\bar{1}$4	2.152		
13$\bar{1}$*	3.401	3.40	11	332	2.115	2.113	11
221	3.254	3.25	12	313*	2.113		
223	3.231			42$\bar{4}$*	2.083	2.084	7
13$\bar{1}$*	3.134	3.13	76	15$\bar{1}$*	2.061	2.061	8
221	3.088	3.08	100	042	2.059		
310	3.082			332	1.950		
3$\bar{1}$0*	2.970	2.969	100	51$\bar{2}$	1.949	1.949	4
113*	2.927	2.925	63	51$\bar{1}$	1.949		
13$\bar{1}$	2.812	2.809	10	513	1.894		
3$\bar{1}$1	2.809			510	1.894		
313	2.807			44$\bar{3}$	1.890	1.892	11
311*	2.782	2.781	26	13$\bar{4}$	1.889		
22$\bar{4}$	2.748	2.748	46	3$\bar{1}$5	1.888		
023*	2.648	2.648	18	006	1.888		
04$\bar{1}$*	2.593	2.593	34	33$\bar{3}$	1.864		
3$\bar{1}$2	2.535	2.535	7	025	1.861		
33$\bar{2}$	2.533			31$\bar{6}$	1.861	1.860	13
33$\bar{1}$*	2.506	2.505	65	35$\bar{2}$	1.861		
24$\bar{2}$	2.428	2.427	10	44$\bar{1}$	1.860		
40$\bar{1}$	2.428			403	1.857		
11$\bar{5}$	2.426			33$\bar{6}$	1.832	1.831	7
400	2.382	2.382	8	51$\bar{2}$	1.832		
330	2.368	2.369	16	44$\bar{4}$	1.830		
42$\bar{2}$	2.312	2.312	4	405	1.830		

[1]Observed values were obtained using a Phillips Diffractometer, employing CuK$_\alpha$ radiation monochromated with a curved graphite crystal. Quartz was used as an internal standard. Indices were obtained for the C-centered unit cell.

*These reflections were used for the refinement of lattice parameters. Where ambiguity exists in the choice of hkl, decisions were made on the basis of intensities as determined using the single-crystal diffractometer.

Refinement

Refinement was carried out using the program RFINE2 of Finger and Prince (1975), employing scattering factors of Doyle and Turner (1968), the weighting scheme of Cruickshank (1965, p. 114), and beginning with the structure parameters of Ohashi and Finger (1975). Reflections having individual discrepancy factors greater than 0.5 were rejected. During the first stages of refinement all of the Mg was assumed to be in the M4 site and the Ca to be in the M5 site, with additional Mn completing the occupancy of these sites, and Mn being exclusively assigned to the M1, M2, and M3 sites. Following the convergence of positional parameter refinement, site occupancies were allowed to vary with both Mn and Mg assigned to M1 through M4, and Ca and Mn assigned to M5. No bulk-chemistry restraints were placed on the occupancy factors. Refinement was completed with refinement of occupancy values, atom coordinates, and isotropic temperature factors. The final R value is 4.8 percent for all data and 4.2 percent excluding rejected data. Structure factors are listed in Table 3,[2] atom coordinates and isotropic temperature factors in Table 4, and site occupancies in Table 6. Selected interatomic distances as calculated using the program ORFFE (Busing *et al.*, 1964) are listed in Table 5 with standard errors calculated from standard errors of unit-cell parameters and the variance-covariance matrix from the final cycle of refinement.

Discussion of cation ordering

The rhodonite crystal structure has been described in detail elsewhere (*e.g.* Peacor and Niizeki, 1963) and will not be further described here. We are principally concerned with the occupancies of the M1–M5 sites. Peacor and Niizeki concluded, on the basis of M–O interatomic distances and peaks in a difference electron-density synthesis, that the Fe and Mg probably occupied the M4 site and that Ca was confined to the M5 site. The formula of rhodonite from the locality serving as a source for the crystal used in that diffraction study was $(Mn_{4.01}Ca_{0.81}Mg_{0.16}Fe_{0.29})(Si_{4.99}Al_{0.02})O_{15.1}$. The coordination polyhedra about M1, M2, and M3 are only slightly distorted octahedra, having average M–O distances of 2.219, 2.215, and 2.229A respectively, in good agreement for occupancy only by Mn. The M4 coordination is highly irregular, however, approaching five-coordination because one of the six M–O distances is 2.88A. Two

[2] To receive a copy of this material, order document AM-78-076 from the Business Office, Mineralogical Society of America, Suite 1000 lower level, 1909 K Street, N.W., Washington, D.C., 20006. Please remit $1.00 for the microfiche.

M4–O distances (1.98 and 2.04A) are the smallest of all M–O distances, and this was good evidence that the smaller Mg and Fe preferentially occupy this site. The more irregular seven-coordinate M5 polyhedron has an average M–O distance of 2.42A, the smallest distance being 2.26A, a reflection of the strong preference of Ca for this site.

Dickson (1975), on the basis of an interpretation of Mössbauer spectra, concluded that most of the Fe in rhodonite is in the M1, M2, M3, and M4 sites, with only a slight preference for the M4 site. He notes that such a large proportion of Fe in M1, M2, and M3 is at variance with the conclusion of Peacor and Niizeki. That Fe does not have a marked preference for M4 was further indicated by the fact that the relative occupancies of Fe in the various sites was the same in both low- and high-Fe rhodonites.

Ohashi and Finger (1975) refined the structure of a rhodonite having formula $Mn_{0.81}Fe_{0.07}Mg_{0.06}Ca_{0.05}SiO_3$, and concluded that M1, M2, and M3 are preferentially occupied by Mn, Mg and Fe prefer M4, and Ca is ordered in M5, although they note that some Ca may also be in M4. All three investigations cited above thus agree that M4 is preferred by Fe (or Mg) and M5 by Ca, although the interpretations differ in detail.

Table 4. Atom coordinates and isotropic temperature factors (standard errors in parentheses)

Atom	x	y	z	B(A^2)
M1	0.00123(6)[a]	0.03004(6)	0.14764(6)	0.70(2)
M2	0.00119(6)	0.12745(6)	0.44535(6)	0.74(2)
M3	0.01589(6)	0.20418(6)	0.73086(6)	0.72(2)
M4	0.05527(8)	0.26488(8)	0.02469(8)	0.93(2)
M5	0.99616(8)	0.35153(7)	0.30258(7)	1.11(2)
Si1	0.2045(1)	0.4487(1)	0.9126(1)	0.72(2)
Si2	0.2121(1)	0.3655(1)	0.6546(1)	0.69(2)
Si3	0.2160(1)	0.5787(1)	0.5302(1)	0.73(2)
Si4	0.2138(1)	0.5061(1)	0.2616(1)	0.74(2)
Si5	0.2069(1)	0.7015(1)	0.1252(1)	0.70(2)
OA1	0.1276(3)	0.0734(3)	0.0390(3)	1.01(4)
OA2	0.1192(3)	0.1585(3)	0.3219(3)	1.02(4)
OA3	0.1151(3)	0.9216(3)	0.4359(3)	1.00(4)
OA4	0.1185(3)	0.0141(3)	0.7324(3)	0.96(4)
OA5	0.1274(3)	0.7895(3)	0.8547(3)	0.93(4)
OA6	0.1005(3)	0.8327(3)	0.1301(3)	0.98(4)
OB1	0.1269(3)	0.3212(3)	0.9046(3)	1.18(5)
OB2	0.1245(3)	0.2342(3)	0.6114(3)	1.05(4)
OB3	0.1273(3)	0.7100(3)	0.5911(3)	1.58(5)
OB4	0.1254(3)	0.3807(3)	0.1835(3)	1.21(5)
OC1	0.1701(3)	0.4672(3)	0.7788(3)	1.02(4)
OC2	0.1602(3)	0.4556(3)	0.5632(3)	1.37(5)
OC3	0.1649(3)	0.5377(3)	0.3875(3)	1.10(4)
OC4	0.1595(3)	0.6426(3)	0.2215(3)	0.98(4)
OC5	0.1465(3)	0.5927(3)	0.9958(3)	0.89(4)

[a]Standard deviations in parentheses in units of final digit shown.

Table 5. Cation–anion interatomic distances (A) (standard errors in parentheses)

M1-OA1	2.182(3)	M2-OA2	2.213(3)
OA1	2.333(4)	OA3	2.242(3)
OA2	2.268(4)	OA3	2.280(3)
OA4	2.253(3)	OA4	2.353(4)
OA5	2.139(3)	OB2	2.150(4)
OA6	2.137(3)	OB3	2.089(4)
ave.	2.219	ave.	2.221
M3-OA3	2.253(4)	M4-OA1	2.090(3)
OA4	2.118(3)	OA5	2.770(3)
OA6	2.392(3)	OA6	2.195(4)
OB1	2.198(4)	OB1	2.026(3)
OB2	2.104(3)	OB4	1.954(4)
OC4	2.234(3)	OC5	2.334(3)
ave.	2.217	ave.	2.228
M5-OA2	2.270(3)	Si1-OA1	1.629(3)
OA5	2.224(4)	OB1	1.590(3)
OB3	2.236(4)	OC1	1.657(3)
OB4	2.239(3)	OC5	1.642(3)
OC1	2.631(4)		
OC2	2.708(4)	ave.	1.630
OC3	2.532(4)		
ave.	2.406		
Si2-OA2	1.613(3)	Si3-OA3	2.613(3)
OB2	1.598(3)	OB3	1.501(4)
OC1	1.655(3)	OC2	1.657(3)
OC2	1.638(3)	OC3	1.626(3)
ave.	1.626		1.622
Si4-OA4	1.617(3)	Si5-OA5	1.597(3)
OB4	1.587(3)	OA6	1.609(3)
OC3	1.632(3)	OC4	1.660(3)
OC4	1.644(3)	OC5	1.659(4)
ave.	1.620	ave.	1.632

The results of our refinement are partially constrained by two assumptions regarding occupancies, namely that all of the available Ca is constrained to M5, and that no Mg occupies this site. We believe that these are reasonable assumptions, based on previous results. The final occupancy factors (Table 6) result in the formula $Mn_{3.54}Mg_{0.86}Ca_{0.60}Si_5O_{15}$, in fair agreement with the results of the electron microprobe analysis, $Mn_{3.73}Mg_{0.73}Ca_{0.51}Fe_{0.03}Si_5O_{15}$. The difference in results lies in higher values for both Ca and Mg in the formula obtained from the refinement.

Table 6. Refined site occupancies

M1	Mn	0.89(1)	M4	Mn	0.53(1)
	Mg	0.11		Mg	0.47
M2	Mn	0.86(1)	M5	Mn	0.40(1)
	Mg	0.14		Ca	0.60
M3	Mn	0.86(1)			
	Mg	0.14			

The M1, M2, and M3 sites are nearly identical in occupancy, having 0.11, 0.14, and 0.14 Mg respectively. This is consistent with their similarity in coordination polyhedra. All three are octahedrally coordinated, with average M–O interatomic distances of 2.219, 2.221, and 2.217A respectively. Individual M–O distances show no major deviations from the average values, while the deviations which do exist are similar for each site. Ohashi and Finger's average M–O distances for M1, M2, and M3 (2.213, 2.228, and 2.217A) and their Mg^{2+} site occupancies (0.07, 0.07, 0.09) are very similar to our results, although their crystal had less than half the Mg of our rhodonite. It should be noted that the rhodonite of Ohashi and Finger ($Mn_{4.05}Fe_{0.35}Mg_{0.30}Ca_{0.25}Si_5O_{15}$) contained substantial Fe in addition to Mn, Mg, and Ca, resulting in some ambiguity in the interpretation of composition as a function of occupancy factors, as indeed they recognized.

The coordination geometry of M4 is consistent with the absence of Ca in that site. Although the average of six M–O distances is 2.228A, nearly identical to the average values for M1, M2, and M3, one value is exceptionally large (2.770A). The M4 coordination polyhedron is nearly five-coordinate, as noted by Peacor and Niizeki (1963). Excluding the one long bond distance results in an average of 2.210A for the remaining five. This is clearly consistent with the site occupancy of $Mn_{0.53}Mg_{0.47}$, determined assuming that no Ca occupies this site.

The very irregular seven-coordinated M5 has a geometry consistent with occupancy by all the available Ca, as verified by the site occupancy refinement. The average M5–O distance is 2.406A, only slightly smaller than that reported by Peacor and Niizeki (2.418A) for a rhodonite with approximately 0.8 Ca per five large cations. Ohashi and Finger reported an average M5–O distance of 2.395A in a rhodonite with 0.25 Ca per five large cations, although their occupancy factor for Ca appears to be consistent with a Ca content even less than that. The average M5–O distance thus appears to be relatively insensitive to variation in the relative proportion of Ca and Mn, despite the significantly smaller radius of the latter. We should note that our value of Ca occupancy (0.60) is very close to that found by the analyses (0.51) and confirms the validity of the assumption used throughout refinement that Ca occupies the M5 site exclusively.

In summation, this refinement has confirmed that Ca preferentially occupies M5, that Mg substitutes in almost equal proportion in M1, M2, and M3, but that there is a marked preference for Mg in M4 by a factor of more than four. These results for Mg contrast with those of Dickson for Fe, in that he showed that although there is a preference for Fe in M4, it is not a marked preference, and the total Fe in M1, M2, and M3 is greater than that in M4. The difference in the substitution roles of Mg and Fe^{2+} appears to relate directly to their ionic radii. Those of Mn^{2+} (0.83A) and Fe^{2+} (0.78A) are more nearly alike, compared with that of Mg^{2+} (0.72A) (Shannon and Prewitt, 1969), resulting in similar occupancies for M1 through M4, despite the fact that there is a preference of Fe^{2+} for distorted sites due to a crystal-field stabilization energy factor.

It might be argued that rhodonites forming at lower temperatures might display a greater degree of order of Mg in M4 than is displayed by this material, which formed at about 600°C. We have determined, however, that the pyroxene with which the rhodonite equilibrated has a submicroscopic exsolution texture and consists of two pyroxenes which have space groups $P2_1/c$ and $C2/c$ respectively. Diffusion of large cations thus occurred in the pyroxene over distances much greater than those necessary for ordering of Mg in the rhodonite. This was presumably a retrograde metamorphic effect, occurring at temperatures well below 600°C. The cation distributions may therefore represent a near-maximum ordering condition in natural samples. Refinement of an Mg-rich rhodonite from a greenschist-facies terrane is needed to confirm this conclusion.

Rhodonite phase equilibria

The Balmat rhodonite appears to be the most magnesian known, with 100 Mg/R^{2+} = 15 percent. Pyroxenoids generally have little magnesium in solution, 95–100 percent of the composition being represented by the components $CaSiO_3$–$FeSiO_3$–$MnSiO_3$. Ohashi *et al.* (1975) plotted rhodonite and pyroxmangite analyses on a diagram with components $CaSiO_3$–$MnSiO_3$–$(Fe,Mg)SiO_3$. They observed that pyroxmangites are less calcic than rhodonite, as also found by Momoi (1974). We have replotted pyroxenoid compositions on this diagram (Fig. 1), considering only pyroxmangites and rhodonites which have been well-characterized. Bustamites, wollastonites, pyroxferroites, and inverted ferrobustamites (see below) are also included for completeness. Some more calcic pyroxmangites which overlap compositionally with the least calcic rhodonites have been reported. Unfortunately these have not yet been adequately characterized by X-ray diffraction and may actually be rhodonite or two-phase mixtures; these have been excluded from Figure 1. The two-phase pyroxenoid pairs of Hodgson (1975) from Broken Hill, of Mason (1973, 1975) from Broken Hill and Franklin, as well

as unpublished material by the writers, have also been plotted to give some feeling for possible miscibility gaps at metamorphic temperatures (estimated to be 650 ± 100°C for all these occurrences). The most Fe-rich rhodonite–bustamite pair from Broken Hill (A, Fig. 1) coexists with manganoan hedenbergite. A ferroan bustamite (B), which has inverted to a hedenbergite–bustamite mixture, is also plotted (Mason, 1973), as well as a ferrobustamite (C) inverted to ferrohedenbergite from Skaergaard (Wager and Deer, 1939). It is clear that bustamites richer in iron than that in assemblage A are less stable than equivalent hedenbergite or hedenbergite + Fe-poor bustamite ± rhodonite at these temperatures. The pyroxferroites (D), which are isostructural with pyroxmangite, are from rapidly-quenched lunar basalts. Experiments of Lindsley and Burnham (1970) suggest that they are metastable with respect to fayalite + silica + hedenbergite at ordinary crustal pressures. The two Mn-rich pyroxmangite–rhodonite pairs are constructed from the data of Ohashi *et al.* (1975) for Japanese materials from Taguchi, Aichi and Watsuka, Kyoto. Ohashi (personal communication) states that the materials are from either end of a single hand-specimen and may be close to equilibrium. The tielines are reasonably consistent with each other and with a possible miscibility gap defined by our unpublished data shown as circled crosses and circled dots.

Rhodonite shows extensive substitution of Fe for Mn, with up to 35 mole percent $FeSiO_3$. In view of Dickson's (1975) conclusions on Fe distribution, it is unclear how much Fe can be accommodated in rhodonite. The Balmat rhodonites have very little iron simply because the rock is low in iron. The maximum Mg possible in rhodonite is also unknown. The Balmat rhodonite coexists with a phase close to $MnMgSi_2O_6$ in composition, fixing the Mg content in the rhodonite by a reaction such as:

Rhodonite + Pyroxene X

$$\rightleftarrows \text{Mg–rhodonite}$$

$$(MnSiO_3)_{ss} + xMnMgSi_2O_6 \rightleftarrows (MnSiO_3)_{1+x}(MgSiO_3)_x \quad (1)$$

or the more complex reaction

Rhodonite + Pyroxene X + Calcite + Quartz

$$\rightleftarrows \text{Mg–rhodonite} + CO_2$$

$$CaMn_4Si_5O_{15} + 4xMnMgSi_2O_6 + 2xCaCO_3 + 2xSiO_2 \rightleftarrows (CaMn_4Si_5O_{15})_{1+x}(CaMg_4Si_5O_{15})_x + 2xCO_2 \quad (2)$$

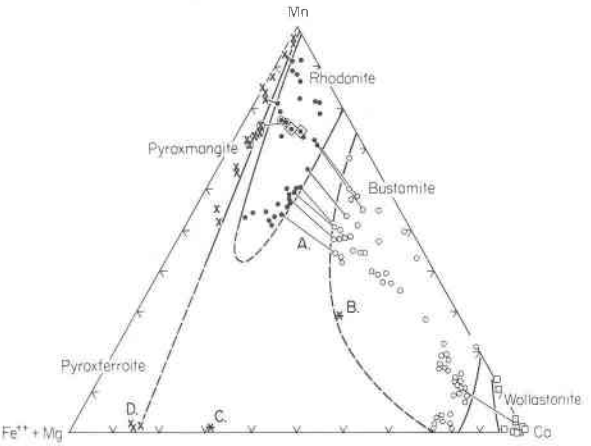

Fig. 1. Plot of pyroxenoid compositions in $CaSiO_3$–$MnSiO_3$–$(Fe+Mg)SiO_3$ space. Coexisting pairs are connected by tielines. Mg–rhodonites are shown by ◈, pyroxmangites and pyroxferroites by x, rhodonites by •, bustamites by ○, wollastonites by ⌊ ⌋, inverted bustamites by *. The ⊗ and ⊙ are unpublished analyses from Franklin, New Jersey. A, B, C, and D are referred to in the text.

The rhodonite from sample number 1 coexists with talc + quartz, and this also fixes $(MgSiO_3)_{ss}$ in rhodonite for the reaction:

Rhodonite + Talc

$$\rightleftarrows \text{Mg–rhodonite} + \text{Quartz} + \text{Vapor} \quad (3)$$

$$(MnSiO_3)_{ss} + xMg_3Si_4O_{10}(OH)_2 \rightleftarrows (MnSiO_3)_1(MgSiO_3)_{3x} + xSiO_2 + xH_2O$$

Any or all of these reactions could fix the Mg content of the rhodonite. However, any quantification must wait until the $MnMgSi_2O_6$ phase is fully characterized. The first reaction is controlled by P–T, the second reaction by P–T–fCO_2 and the third by P–T–fH_2O. The nature of these reactions suggests that the Mg content of the Balmat rhodonite may be close to the maximum possible in a naturally occurring phase, however. It should be noted that Wang (1936) reported the occurrence of a high-magnesian rhodonite-like phase which he called hsihutsunite. His analysis is subject to question, however, because when normalized to 5 Si it yields 5.86 octahedrally-coordinated cations, a value much in excess of that required for the rhodonite structure.

An examination of the experimental petrology literature would suggest that the stability of rhodonite in P–T–X space is well known (Maretsch and Mottana, 1976; Peters, 1971). However, it should be noted that the solid solutions exhibited by rhodonite have important implications for its stability in structural transformations as well as solid–solid and decarbonation reactions. The small ΔS, ΔV, ΔH, and ΔG changes accompanying a solid–solid reaction

mean that substituting ions (Mg,Ca) will have a large effect on the experimentally-determined equilibrium P–T relations. Application of Maretsch and Mottana's data on the rhodonite–pyroxmangite transformation should allow a maximum pressure to be assigned for a given temperature, inasmuch as the pyroxenoid present is rhodonite and not pyroxmangite. Direct application of their data yields the not surprising conclusion that $P < 12$ kbar at 600°C. However, since the effects of substitution (*i.e.* Mg/Mn or Ca/Mn) on the transformation are unknown, it is not possible to quantitatively shift the curve to apply to the natural compositions. An examination of ionic radii suggests that the addition of Mg will stabilize pyroxmangite, whereas Ca will stabilize rhodonite. Whether the net effect of these opposed shifts will yield a more instructive pressure limit than <12 kbar remains to be experimentally determined.

Peters (1971) has located the decarbonation reaction for rhodochrosite plus quartz at 2 kbar. He found that for the calcium-free system pyroxmangite and not rhodonite was formed. Natural bulk compositions may shift the rhodonite–pyroxmangite transformation enough to change the pyroxenoid produced by the breakdown of rhodochrosite + quartz, and allow an estimate of X_{H_2O}/X_{CO_2} to be made for the assemblage rhodonite + quartz + carbonate. Even in this case, modeling the reaction would be difficult without knowing the activity–composition relations in the carbonate and rhodonite phases. Qualitative examination of probable shifts in the decarbonation reaction suggests that rhodonite is stable at relatively low X_{CO_2}, consistent with the estimates of Valley and Essene (1976) for the Adirondack marbles in general. Further careful experiments are needed in the system CaO–MnO–SiO_2–CO_2–H_2O to quantify these equilibria for natural impure compositions. Incautious application of experimental equilibria data on $MnSiO_3$ to natural impure rhodonites without proper consideration of the impurities and their distribution within the structure may lead to serious errors.

Acknowledgments

We thank Professor W. C. Bigelow, Larry Allard, John Mardinly and Peggy Hollingsworth of The University of Michigan Microprobe Laboratory for continuing help and upkeep of the electron microprobe. We are grateful to St. Joe Minerals Corporation who provided summer support for one of us (Philip E. Brown), and particularly to Dave Dill who saw that the rhodonite-bearing sample was saved. This research was supported in part by a Sigma Xi Grant-in-Aid of Research to Philip E. Brown and NSF grant EAR 75-22388 to Eric J. Essene.

References

Brown, P. E., E. J. Essene and W. C. Kelly (1978) Sphalerite geobarometry in the Balmat-Edwards district, New York. *Am. Mineral., 63,* 250–257.

Busing, W. R., K. O. Martin and H. A. Levy (1964) A Fortran crystallographic function and error program. *U.S. Natl. Tech. Inform. Serv. ORNL-TM-306.*

Cruickshank, D. W. J. (1965) Errors in least squares methods. In J. S. Rollett, Ed., *Computing Methods in Crystallography.* Pergamon Press, Oxford.

Dickson, B. L. (1975) The iron distribution in rhodonite. *Am. Mineral., 60,* 98–104.

Doyle, P. A. and P. S. Turner (1968) Relativistic Hartree-Fock X-ray and electron scattering factors. *Acta Crystallogr., A24,* 390–397.

Finger, L. W. and E. Prince (1975) A system of Fortran IV computer programs for crystal structure computations. *Natl. Bur. Stand. (U.S.) Tech. Note, 854.*

Hodgson, C. J. (1975) The geology and geological development of the Broken Hill Lode, in the New Broken Hill Consolidated Mine Australia, Part II: Mineralogy. *J. Geol. Soc. Aust., 22,* 33–50.

Lindsley, D. H. and C. W. Burnham (1970) Pyroxferroite: stability and X-ray crystallography of synthetic $Ca_{0.15}Fe_{0.85}SiO_3$ pyroxenoid. *Science, 168,* 364–367.

Maretsch, W. V. and A. Mottana (1976) The pyroxmangite–rhodonite transformation for the $MnSiO_3$ composition. *Contrib. Mineral. Petrol., 55,* 69–79.

Mason, B. (1973) Manganese silicate minerals from Broken Hill, NSW. *J. Geol. Soc. Aust., 20,* 397–404.

——— (1975) Compositional limits of wollastonite and bustamite. *Am. Mineral., 60,* 209–212.

Momoi, H. (1974) Hydrothermal crystallization of $MnSiO_3$ polymorphs. *Mineral. J., 7,* 359–373.

Ohashi, Y. and L. W. Finger (1975) Pyroxenoids: a comparison of refined structure of rhodonite and pyroxmangite. *Carnegie Inst. Wash. Year Book, 74,* 564–569.

———, A. Kato and S. Matsubana (1975) Pyroxenoids: a variation in chemistry of natural rhodonites and pyroxmangites. *Carnegie Inst. Wash. Year Book, 74,* 561–564.

Peacor, D. R. and N. Niizeki (1963) The determination and refinement of the crystal structure of rhodonite, $(Mn,Ca)SiO_3$. *Z. Kristallogr., 119,* 98–116.

Peters, T. (1971) Pyroxmangite: stability in H_2O–CO_2 mixtures at a total pressure of 2000 bars. *Contrib. Mineral. Petrol., 32,* 267–273.

Shannon, R. D. and C. T. Prewitt (1969) Effective ionic radii in oxides and fluorides. *Acta Crystallogr., B25,* 925–946.

Valley, J. and E. J. Essene (1976) Calc-silicate reactions in Grenville marble, N.Y. *Geol. Soc. Am. Abstracts with Programs, 8,* 1151.

Wager, L. R. and W. A. Deer (1939) *Geological Investigations in East Greenland:* Pt. III. *Medd. om Grönland 105.*

Wang, C. C. (1936) The rhodonite veins of Hsihutsun, Changpin district, north of Peiping. *Geol. Soc. China Bull., 15,* 87–104

Manuscript received, July 20, 1977; accepted for publication, March 31, 1978.